Published in final edited form as:
J Mol Biol. 2010 March 12; 396(5): 1346–1360. doi:10.1016/j.jmb.2009.12.059.

A Folding Zone in the Ribosomal Exit Tunnel for Kv1.3 Helix Formation

LiWei Tu and **Carol Deutsch**
Department of Physiology, University of Pennsylvania, Phila., PA 19104-6085

SUMMARY

Although it is now clear that protein secondary structure can be acquired early, while the nascent peptide resides within the ribosomal exit tunnel, the principles governing folding of native polytopic proteins have not yet been elucidated. We now report an extensive investigation of native Kv1.3, a voltage-gated K^+ channel, including transmembrane and linker segments synthesized in sequence. These native segments form helices vectorially (N- to C-terminus) only in a permissive vestibule located in the last 20Å of the tunnel. Native linker sequences similarly fold in this vestibule. Finally, secondary structure acquired in the ribosome is retained in the translocon. These findings emerge from accessibility studies of a diversity of native transmembrane and linker sequences and may therefore be applicable to protein biogenesis in general.

Keywords

Protein folding; nascent peptides; potassium channel biogenesis; transmembrane Kv segments; folding zone in the ribosome tunnel; PEG-MAL; α-helix

INTRODUCTION

The ribosomal tunnel has a length of ~100Å from the peptidyl transferase center (PTC) to the exit site and an average diameter of ~15Å[1]. This tunnel hosts protein synthesis and participates in folding the nascent peptide2–5. Moreover, this participation by the tunnel is differentially specified along the 100 Å length of the tunnel4. Some helical sequences compact near the exit port[2, 3, 5–9] and a few helical sequences in non-native contexts, including polyalanines and a transmembrane segment inserted into preprolactin, compact near the PTC4, [5]. Polyalanines may be exceptional because alanine has a high helix propensity and possesses the smallest alkyl side-chain of all amino acids. However, key questions remain unanswered, particularly for polytopic proteins. Namely, do these observations hold for all native sequences (with larger side-chains) in their native context in the tunnel during their sequential synthesis? Whereas changes in folding of a native membrane segment from aquaporin in the tunnel can affect the location of the nascent chain in the translocon[10], there is relatively little information regarding the influence of consecutive transmembrane sequences on peptide folding in the ribosomal tunnel during the sequential synthesis of a polytopic protein.

Corresponding Author: Carol Deutsch Department of Physiology University of Pennsylvania Phila., PA 19104-6085 Phone: 215.898.8014 Fax: 215.573.5851 cjd@mail.med.upenn.edu.

To investigate this issue systematically, we chose to probe the folded status of different regions of a polytopic protein, Kv1.3, a human voltage-gated potassium (Kv) channel. Crystal structures of highly homologous mature Kv channels (Kv1.2 and a chimera Kv1.2/2.1) have been solved[11, 12]. Moreover, we have previously probed select areas of Kv1.3 in the context of their native sequences and shown that helical regions in the crystal structure compact inside the ribosomal exit tunnel[2, 3, 6]. Specifically, the N-termini of the native transmembrane segments S1 and S6 form helices in the last 20Å of the tunnel near the exit port. But S1 does not compact near the PTC[6]. With this limited knowledge of Kv folding, we set out to investigate whether the remaining transmembrane segments and linkers of Kv1.3 fold inside the tunnel, and if so, in which regions of the tunnel. Is there a common region or zone in the tunnel that supports secondary folding of Kv1.3? Moreover, we can ask whether secondary folding is cooperative. For example, in a polytopic protein, does folding of a transmembrane segment require the presence (folded or unfolded) of its adjacent downstream or upstream transmembrane segment? Our knowledge is similarly limited regarding the structure of linkers between the transmembrane segments during biogenesis. Their folding in the tunnel may also be influenced by flanking transmembrane segments.

In this paper, we report the biogenesis of secondary structure of transmembrane segments of Kv1.3 and the intervening linkers. For the first time, we describe the sequence of events by which a succession of transmembrane segments forms helices. Using a combination of accessibility assays, both cysteine pegylation[3, 6] and N-linked glycosylation[7], we have identified which helices form in the exit tunnel, the tunnel location of compaction, and whether those segments that form helices in the tunnel retain their compact structure during elongation and subsequent movement through the translocon.

The following conclusions for folding of nascent Kv1.3 sequences within their native contexts may be derived from our results. First, helical transmembrane sequences initially compact only inside the distal 20Å vestibule of the ribosomal tunnel near the exit port. Helix formation for most Kv1.3 transmembrane segments thus occurs vectorially from N- to C-terminus as each segment moves sequentially into the vestibule. Second, helical linker sequences also form compact structures inside this vestibule and in the absence of helix formation of their C-terminal flanking transmembrane segments. These two findings define the vestibule as a region for Kv1.3 helix formation. Third, helical structures, whether transmembrane or linker segments, formed in the tunnel retain their helicity in the translocon. These conclusions emerge from a diversity of native transmembrane and linker sequences that comprise Kv1.3 and therefore may be applicable to protein biogenesis in general.

Results

To guide our investigation of secondary folding of polytopic proteins in the ribosome-translocon complex, we used Kv1.3, which is highly homologous to a chimeric voltage-gated potassium channel, Kv1.2/2.1[12], whose crystal structure is known and is shown in Figure 1 (two subunits only). This is the structure of the mature channel found in the plasma membrane. All 6 transmembrane segments (S1–S6) are helical, and small helices are present in several linking sequences. Are these secondary structures already manifest in the ribosomal tunnel early in biogenesis, and if so, in which regions of the tunnel? Are there multiple such folding regions within the ribosomal tunnel, or just one for the diverse helical sequences from Kv1.3? To address this, we engineer cysteines, one at a time, in the nascent peptide and evaluate its ability to be covalently modified by a high molecular-weight maleimide. The adduct can be detected as a shift in mobility of the peptide on a protein gel. We have used this mass-tagging cysteine accessibility assay[2, 3, 6] previously to characterize secondary structure acquisition of the cytosolic N-terminal domain (T1), the cytosolic T1-S1 linker, and S1 located in the ribosomal tunnel[2, 6]. This cysteine scanning approach allows us to examine the secondary

structure of defined segments of the nascent peptide. Key to this strategy is the use of a molecular tape measure, i.e., a nascent peptide known to be all-extended, and a cysteine scan of the tape measure3. The extent of cysteine labeling by polyethyleneglycol maleimide (PEG-MAL) depends on the distance from the PTC to each individual cysteine. The tape measure was positioned to span the length of the ribosomal exit tunnel using the appropriate restriction enzyme and then modified with PEG-MAL (pegylated). Tape-measure cysteines that are only 26 amino acids from the PTC are relatively inaccessible to PEG-MAL. As the target cysteine is moved increasingly further than 26 residues from the PTC, labeling increases monotonically. Those residues that are ≥ 33 amino acids from the PTC are ≥80% labeled with PEG-MAL. Thus, to completely emerge from the ribosomal exit tunnel, a given residue in an extended conformation is ~33 amino acids from the PTC3. For an all-extended peptide, this corresponds to a distance of ~99–112Å, in excellent agreement with anatomical dimensions derived from structural studies1. We refer to this distance as the operational length of the ribosomal tunnel.

We chose to study Kv1.3 biogenesis in a nascent peptide that lacks the T1 domain (Kv1.3 in which residues 1–141 have been deleted (ΔT1)) to avoid the possibility of blocking access to the tunnel by the folded T1 domain. This deletion does not influence folding of downstream sequences inside the ribosomal tunnel[6]. Nor does it disrupt function of the mature channel13, 14.

We have previously shown that the N-terminal portion of S1 compacts differentially along the ribosomal tunnel in the absence of ER membranes[6]. Therefore, we began our investigation of Kv1.3 structure formation in free ribosomes by probing, in order, the transmembrane segments. The N-terminal portion of S1 forms an α-helix only in the distal portions of the ribosomal tunnel within the last ~20Å of the exit port whereas the C-terminal portion of S1, located in the middle of the tunnel, remains extended[6]. Moreover, the C-terminus of S1 located near the PTC is also extended. We therefore asked whether the C-terminal portion of S1 compacts elsewhere in the tunnel. To address this question, we positioned the C-terminus of S1 in the distal portion of the tunnel to test whether in this new location, a putative zone for secondary folding[4], it would compact. We linearized a DNA template of Kv1.3ΔT1 with a restriction enzyme (*Ppum*I) at the site indicated in Figure 2A (residue 231). The mRNA transcribed from this DNA template lacks a stop codon; thus translation of the mRNA produces an arrested nascent peptide that remains attached to the ribosome at the PTC, at residue 231, thus mimicking a translation intermediate. Consequently, the *Ppum*I-cut nascent peptide positions the C-terminus of S1 inside the bottom part of the tunnel and the C-terminal S1–S2 linker resides near the PTC (Figure 2C, right). A cysteine scan, one at a time, along the nascent peptide residing inside the tunnel, specifically at residues 191, 195, 197, and 200, (indicated as filled black squares, Figure 2A) was carried out using standard mutagenesis. These constructs were independently studied using a cysteine accessibility assay to determine the location of each cysteine relative to the PTC[3]. A peptide that has been mass-tagged with PEG-MAL (covalent S-C bond) can be detected on a gel as a 10 kD or larger shift in mobility[3]. Because a fully extended peptide occupies 3.0–3.4 Å per amino acid whereas an α-helix occupies 1.5 Å per amino acid, the length of the peptide when the modifiable cysteine first emerges from the ribosome at the exit site reflects the compactness of the nascent peptide.

Because the pegylation assay determines reactivity/accessibility of nascent chain sites near the end of the tunnel or after they emerge, the following assumptions underlie the interpretation of the results. First, the slope of the plot of fraction pegylated versus distance from the PTC to a given cysteine (ΔPTC) reflects the number of residues per angstrom. Second, if the slope is ~0.5 that observed for an all-extended peptide, then this could reflect the presence of an α-helix, but does not preclude the presence of several dynamic states with an ensemble average relative slope of 0.5.

The assay is shown in Figure 2B for each cysteine-containing construct. The first lane shows a ~ 11kD peptide. This is the unpegylated parent peptide (labeled "0"). Lanes 2–7 show the extent of pegylation (labeled "1") after incubation with PEG-MAL for 3 or 5 hrs for each cysteine construct. The final extent of pegylation was reached within 3 hours. Quantification of the pegylation gels is shown in Figure 2C (open triangle, red line), along with the results for an all-extended molecular tape measure (filled circles, black line) that was previously calibrated and validated as a standard[3, 6]. A comparison of the fraction labeled for an unknown peptide and the fraction labeled for the tape measure indicates whether the unknown peptide has compact secondary structure. A decrease in slope and/or a shift of the curve to the right for the unknown peptide indicates compact secondary structure within the scanned region of the peptide. Thus, the shallower slope of the scanned C-terminal region of S1 (Figure 2C) indicates that the C-terminal region of S1 is compact (likely helical) in this location within the last 20Å of the tunnel. In regions of the tunnel that are more proximal to the PTC, however, the C-terminal region of S1 is extended[6]. These results suggest that for S1, both N-terminal and C-terminal portions, the equilibrium between the unfolded and folded species is shifted toward the folded state only in the distal region (the last 20Å) of the tunnel but not near the PTC.

To determine whether S2 acquires secondary structure in the ribosomal exit tunnel, we positioned S2 in two different locations suggested to be folding zones[4, 5]. The first location is near the PTC and the second is near the exit port (Figure 3A). In the first case, we created a restriction site at residue 264 and introduced a cysteine at 232 (S232C). S232C is located 33 residues (itself included) from the PTC and is pegylated comparably to the tape measure (dominant band is the pegylated band in Figure 3B, lanes 2–3; red circle (arrow) in Figure 3C). Thus, S2 in this location in the tunnel is not compact. We then relocated the N-terminus of S2 to the last 20Å of the tunnel by engineering a restriction site at position 276, and introduced cysteines at 241, 244, 249, and 251. In this construct, the S2–S3 linker was located near the PTC. Pegylation for residues 244C (ΔPTC 33, mostly pegylated) and 249C (ΔPTC 28, mostly unpegylated) are shown in Figure 3B (lanes 5–8). The fraction pegylated for each engineered cysteine is plotted in Figure 3C (blue circles, blue line) along with the all-extended tape measure (black circles). The fraction pegylated for S2 is coincident with the tape measure, confirming that S2 is extended when it spans the bottom half of the tunnel. Previous mutagenesis and electrophysiological studies[15, 16], as well as crystal structures[11, 12], indicate that S2 is helical in the mature Kv channel. This raises the possibility that S2 acquires its helical structure in a more distal location.

To further probe the folding location for S2, we tested whether the C-terminal region of S2 might compact when it is located near the exit port and the N-terminus has already emerged from the tunnel. We therefore engineered S2 so that its C-terminus resided inside the last 20Å of the tunnel and its N-terminus was outside the tunnel. This nascent peptide was made by creating a restriction site at 291 (Figure 3A). Cysteines were introduced at 246, 252, 258, and 264 and the peptide pegylated to give the data shown in Figure 3B for 246C (ΔPTC 46, mostly pegylated) and 258C (ΔPTC 34, mostly unpegylated) (lanes 9–13) and in Figure 3C (green triangles) for each of the four cysteines. The shallow slope of the pegylation curve for the scanned C-terminus of S2 indicates that it compacts within the last 20Å of the tunnel when its N-terminus has emerged from the tunnel, in contrast to the extended conformation of S2 when S2 resides entirely within the tunnel.

We may draw two additional conclusions from the above experiments. The 10 residues flanking the C-terminus of S2 and immediately proximal to the PTC comprise the S2–S3 linker (residues 265–275). They are also extended in the immediate proximity of the PTC because residues 241 and 244, which are 36 and 33 residues, respectively, from the PTC in the 276-cut construct, are maximally pegylated. However, the extended S2–S3 linker immediately proximal to the

PTC lacks its native C-terminal transmembrane segment, S3, and might yet compact at a more distal location in the tunnel and/or in the presence of S3 (see below). Similarly, the C-terminal portion of the S1–S2 linker is extended in the last 20Å of the tunnel based on the observation that residue 232 is maximally pegylated when ΔPTC is 33 in the 264-cut construct (Figures 3B and C).

The next transmembrane segment probed was S3. The pegylation results in Figure 3C indicate that the 27 residues that include the S2–S3 linker and the N-terminus of S3, located near the PTC (291-cut construct), are coincident with the extended tape measure, i.e., are extended. To probe another tunnel location, we engineered a restriction site at 315 to position S3 in the distal portion of the tunnel (Figure 4A). Cysteines were introduced at residues 275, 279, 283, and 287. Pegylation of these residues (e.g., 275C (ΔPTC 41) and 287C (ΔPTC 29) in lanes 2–5, Figure 4B) is less than that for the tape measure at corresponding ΔPTC-Cys distances. A similar decrease in the slope of the pegylation curve was observed (red triangles, Figure 4C), indicating that the N-terminus of S3 is compact. In addition, we note that the intersection of the S3 curve with the tape measure occurs at a ΔPTC of ~ 27 without a shift of the whole curve to the right. This indicates that the region from the middle of S3 (residue 288) to the middle of S4 (315), which is near the PTC, is extended.

The major voltage sensing segment in Kv channels is the S4 transmembrane segment[17, 18]. To determine its status in the tunnel, we used a restriction site at residue 343 and probed cysteines engineered at 301, 310, and 316 (Figure 4A). Pegylation is similarly decreased relative to the tape measure (Figures 4B and 4C, cyan squares). The N-terminus of S4 compacts in the distal portion of the tunnel as does the immediate N-terminal flanking sequence. This is in agreement with the helix observed for S4 and its N-terminal flanking sequence in the crystal structure of the mature chimeric Kv1.2/2.1 structure[12].

A similar cysteine scan of S5, using the appropriate restriction sites (Figure 4A), indicates that this transmembrane region is compact in the tunnel, again in the distal part of the tunnel near the exit port (Figures 4B and 4C (green diamonds)). Finally, S6 was reported previously to be helical in the distal portion of the tunnel[3].

Compared to the all-extended tape measure, the slope from the pegylation curve of the typical α-helix is 0.44~0.5 (3.0~3.4Å/amino acid vs 1.5 Å/amino acid). The relative average slope for compacted nascent peptides observed from our cysteine scans of S1–S5 is ~0.4, slightly more compact than predicted for an α-helix. One possibility is a kink/bend may exist in the region scanned. Prolines and glycines are present in several of the sequences studied. For example, the kink reported for S3 in a mature Kv channel11, 12, 16 due to a proline in the middle of S3 (corresponding to P286 in Kv1.3), might already be manifest in the orientation of the peptide in the tunnel, producing a more compact arrangement of this portion of S3 in the tunnel. Another possibility is that adjacent side chains may sterically influence the position of a cysteine side chain, especially in an α-helix. Nonetheless, this observed level of compaction (relative pegylation slope of ~0.4) is consistent with our conclusions that transmembrane segments from Kv1.3 form α-helices only in the last 20Å of the exit tunnel. We refer to this tunnel location as a permissive vestibule.

Linker Segments

Having determined the site of secondary structure formation for the native transmembrane segments S1–S6, we then turned to understanding the status of non-membrane segments, namely, the linkers between these transmembrane segments, in the tunnel. Do they fold within the vestibule used by transmembrane segments? To address this question, we focused on the voltage sensor domain (S1–S4). Previously, it was shown that within this voltage sensor, S2–S3–S4 form a cooperative biogenic unit for membrane insertion[19–21]. If the intervening linkers

contribute to this process, then this implies a role for the linkers in cooperative transmembrane folding. According to the crystal structure of the mature Kv1.2/Kv2.1 chimera, some of the Kv linkers contain small helical segments, but the spatiotemporal acquisition of this helicity is unknown. Do they form helical structures early in biogenesis, and if so, do they compact inside the permissive vestibule? To determine secondary structure formation of the intervening linkers relative to their flanking transmembrane segments, we cysteine scanned and pegylated the S2–S3 and S3–S4 linkers.

We engineered a restriction site at residue 305, thereby positioning the S2–S3 linker in the vestibule and S3–S4 linker near the PTC (Figure 5A). A cysteine scan of this nascent peptide was carried out using mutations F271C, N274C, I275C, and N277C, which are 35, 32, 31 and 29 residues, respectively, from the PTC. The fraction pegylated for residue 271C is 0.62 ± 0.03 (Figure 5B, lanes 2–3, and Figure 5C, green circles), which is markedly less than that predicted for the tape measure at this location from the PTC. Residues 274C and 275C are pegylated only 0.43 ± 0.01 and 0.36 ± 0.01, respectively, both much less than the corresponding tape measure residues. Residue 277C is mostly unpegylated (Figure 5B, lanes 4–5) and coincides with the tape measure at this ΔPTC-Cys distance. The slope of the curve is ~ 0.5 of the tape measure slope, consistent with formation of an α-helical structure. Similarly, the link between S3 and S4 was probed using constructs engineered with residue 330 at the PTC and cysteines at positions 295, 298, or 301, which are 36, 33, and 30 residues, respectively, from the PTC. A scan of these residues (Figures 5A and B, lanes 7–10) defines the linker between S3 and S4, which is compact (blue triangles, Figure 5C), consistent with the helical segment modeled by Long et al. for the Kv1.2/2.1 chimera crystal structure[11]. Another conclusion may be drawn from the results shown in Figure 5C. Namely, the fraction of pegylation for residues 277, in the S2–S3 linker, and 301, in the S3–S4 linker, exactly coincides with the fraction pegylated in the tape measure at the identical ΔPTC. Thus, the S3–S4 linker and S4 are extended inside the tunnel near the PTC (as is the S2–S3 linker, see Figure 3) and only compact in the vestibule near the exit port.

In addition to the small helices modeled in the S2–S3 and S3–S4 linkers of the chimera crystal structure, Long et al.[11] also report a short helical segment in the S1–S2 linker. In Kv1.3, the linker connecting transmembrane segments S1 and S2 is 39 residues long and contains a site that is glycosylated in the mature channel protein. To probe this region, we positioned the linker in different tunnel locations with the C-terminus of the linker located successively more distal from the PTC. We engineered restriction sites at 240, 248, and 256 (Figure 6A) and cysteine mutations F207C in the 240-cut peptide, Y213C and S216C in the 248-cut peptide, and E223C and A224C in the 256-cut peptide. Residue F207C, which is 34 residues from the PTC (at site 240), was ~75% pegylated (open diamond, Figure 6B). Similarly, S216C, located 33 residues from the PTC (at site 248), and E224C, located 33 residues from the PTC (at site 256) are each pegylated comparably to the tape measure at the respective distance from the PTC (open square and open inverted triangle, respectively, Figure 6B). Each of the three selected residues is maximally pegylated. A similar fraction labeled was found for residue E223C in the 256-cut construct and Y213C in the 248-cut construct (data not shown). These pegylation results, combined with those from Figure 3, suggest that the S1–S2 linker does not compact inside the tunnel. A single α-helical turn would shorten the ΔPTC-Cys distance by ~7Å, resulting in a maximum fraction pegylated of ~0.5 for a cysteine located 33 residues from the PTC[4]. However, the fraction pegylated is ~0.72, comparable to the all-extended tape measure. Thus, at most, only a small bend or kink (due to the presence of prolines and/or glycines) may be present in the S1–S2 linker region inside the tunnel. The S1–S2 linker, including residues 203–240, is fully extended.

These results are in agreement with those derived from N-glycosylation scanning studies of Kv1.222, which indicate that the S1–S2 linker region is mostly a random coil lacking helical

structure. In the chimeric channel Kv1.2/Kv2.1, however, the middle of the S1–S2 linker manifested a short α-helix in the crystal structure[12]. However, this chimera lacks a glycosylation site that is present in Kv1.3 (N227). In Kv1.3, the fraction of pegylation is independent of the presence of N227 (N227/224C: 0.72 ± 0.04, n = 3; N227Q/224C: 0.72 ± 0.01, n = 3). Thus, the S1–S2 linker in Kv1.3 is extended regardless of whether the aspargine in the glycosylation consensus sequence is present or substituted with glutamine. The linker may acquire some helical character at later stages in biogenesis (see Discussion).

The pegylation results for the cysteine scan of the S1–S2 linker also suggest that the N-terminus of S2 is extended when located in the region of the tunnel near the PTC. In the constructs used in the experiments shown in Figure 6, a portion or most of S2 is in the tunnel near the PTC (red line in Figure 6C cartoons, residues 242–256), yet pegylation of the reporter cysteine is maximal, indicating no compaction has occurred for any segment of the peptide between the PTC and the reporter cysteine, including S2. Thus, the N-terminus of S2 is extended all along the tunnel (see Figure 3).

While we cannot exclude the possibility that a translocon bound to a ribosome will induce conformational changes within the tunnel and/or the nascent peptide that may influence the region of folding, our results demonstrate that helical sequences from Kv1.3 transmembrane and linker segments compact only in the distal vestibule. This vestibule may be a preferred region for folding for other nascent peptides as well.

In the Translocon

Having shown that S2, S3, S4, S5, S2–S3 linker and S3–S4 linker likely form helices only when located in the permissive vestibule near the exit port of the tunnel, we then asked whether these segments remain compact during further chain elongation and entry into the translocon. We chose to use a glycosylation mapping assay[23] to assess the folded status of the nascent peptide sequences in the ribosome-translocon complex by measuring the minimum number of residues required to bridge the distance between the native glycosylation site (N227) and the PTC site. Oligosaccharyltransferase (OST), which is associated with the translocon complex on the luminal side of the ER membrane, glycosylates nascent peptides on an asparagine in a NXT/S motif as the peptide is translocated across the ER membrane and emerges from the translocon with a sufficient number of flanking residues. In our experiments, the glycosylated residue is N227, a native residue located in the linker between S1 and S2 that is glycosylated in the mature Kv1.3. We determined the extent of N227-glycosylation as a measure of emergent length of the peptide from the translocon. If the nascent peptide remains extended in the translocon, then a length of ~66 residues will suffice to permit glycosylation[7, 23]. If a helix forms, e.g. as shown by von Heijne and co-workers for 17 polyAla and 17 polyLeu, then ~74 amino acids will be required to traverse the translocon[7, 8, 23]. Again, it is the *emergent* length of the modifiable residue (in this case asparagine, whereas in the pegylation assay, it is the modifiable cysteine) that will indicate secondary structure.

We made a series of nascent peptides designed to place S2 at different locations in the ribosome-translocon complex with different distances between the PTC and N227 (ΔPTC-N227), and fractionated the translation products on NuPAGE gels to evaluate the fraction of peptide glycosylated (Figure 7A). The gels indicate unglycosylated (lower band in each lane) and glycosylated (upper band with an asterisk in each case) protein. To optimize OST activity, we translated mRNA at 27°C for 50 min, which necessitated screening for possible released peptide at this slightly higher temperature (compared to 22°C). We therefore pre-treated samples with dodecylmaltoside ($C_{12}M$) before collecting the pellets (lane 2, 4, and 6, Figure 7A). If a small amount of peptide had been released into the ER membrane, then $C_{12}M$ treatment of these released peptides would result in their solubilization. Upon centrifugation, these released, solubilized peptides would remain in the supernatant. Thus, the final pellet

reflects only those peptides still attached to the ribosome. The length-dependent fractional glycosylation was quantified and is shown in Figure 7B for peptides of the indicated ΔPTC-N227 length. If S2 is extended inside the translocon, then for peptides with a ΔPTC-N227 length of 79 and 89 amino acids we expect to observe glycosylation of ~60%, according to control values (open circle, Figure 7B). However, in the range of ΔPTC-N227 distances of 79–89 amino acids, these nascent peptides displayed ~30% glycosylation, whereas peptides with a ΔPTC-N227 distance ≥ 99 amino acids was ~60% glycosylated. This is the maximal value for glycosylation, as longer peptides (ΔPTC-N227 = 300) show ~60–65% glycosylation (data not shown). This maximum is comparable to the fractional glycosylation observed for an all-extended control peptide (open circle, Figure 7B) and an appropriately long enough compact control peptide (17 polyLeu, open square) derived from the studies of von Heijne and co-workers. We suggest that a length of >99 residues required to efficiently glycosylate N227 indicates that segments compacted in the tunnel vestibule remain compact in the translocon, consistent with FRET measurements from the Johnson laboratory showing that a single transmembrane segment compacted in the tunnel remains so in the translocon[4, 5].

The following analysis supports this conclusion. Because 66 extended residues are required to span the region between the PTC and OST, the distance is ~ 200 Å[7, 23]. In the 305-cut construct, residue 305 is at the PTC, followed (in order) by the S3–S4 linker and S3 (276–305), the S2–S3 linker (266–275) in the tunnel, and finally, S2 (242–265) and the S1–S2 linker (227–241) in the translocon, a total of 79 residues (Figures 5 and 7C). In this construct, if secondary structures acquired in the tunnel are retained, then a total of 36 residues will be compact and 43 extended. N227 would therefore reside ~183Å (equivalent to ~61 extended amino acids) from the PTC and thus be inaccessible to the OST. Our data are consistent with S2 and the S2–S3 linker remaining compact in the ribosome-translocon complex. If S2 and the S2–S3 linker were extended, then the total distance between the PTC and N227 would be ~237Å (equivalent to ~79 extended residues), leading to maximal glycosylation. This is not observed. Thus, compact regions appear to be retained.

Similarly for 315-, 325-, and 330-cut peptides,), if transmembrane segments S2, S3, and the S2–S3 linker retain their putative helical structure inside the translocon, then specific predictions can be made by an analogous analysis. We calculate that the ΔPTC-N227 distance in equivalent extended residues is ~64, 72, and 74, respectively. We therefore predict that the 315-cut construct will be relatively unglycosylated and the 325- and 330-cut constructs glycosylated ~60%. These predictions are consistent with the results from glycosylation assays, suggesting that the S2 and S3 segments and the S2–S3 linker, putatively helical in the tunnel, remain compact in the translocon.

Yet another inference may be made from our glycosylation studies of the 330-cut construct. S4, located proximal to the PTC, in the presence of microsomal membranes (translocon), is extended. If S4 were also compact at this position, then the distance between the PTC and N227 would be ~180Å (equivalent to ~60 extended residues) and thus N227 would be inaccessible to the OST. This was not the case because N227, in this construct, was glycosylated >60%. Furthermore, chain elongation from 325 to 330 residues produces a slightly increased fraction glycosylated, also indicating that S4 near the PTC of a membrane-bound ribosome, is extended. Pegylation results (Figure 5) already suggest that S4 at this tunnel location, in the absence of membranes, is extended. Thus, the extended structure observed for S4 at this location, does not depend on the presence or absence of ER membranes, i.e., on the presence or absence of the translocon.

We do not know the mechanism underlying the observed compaction in the ribosome-translocon complex and cannot exclude several alternative explanations including the possibility that S3 begins to invert its orientation relative to the bilayer and therefore retains

more nascent chain inside the ribosome and/or translocon. However, the results for the 330-cut peptide eliminate the possibility that S3 is *totally* inverted at this stage. This would result in submaximal glycosylation. Two additional scenarios might explain our results. First, it is possible that the translocon alters the tunnel and/or the structure of the peptide in either location, e.g., shifts the equilibrium between folded and unfolded peptide conformations. Second, S2 may lose its helical structure inside the translocon while the extended S3 becomes compact near the PTC. However, to date, there is no experimental evidence to support the latter scenario.

Given these caveats, we present models based on the results of Figures 3–7B, to depict the likely position and secondary structure of transmembrane and linker regions in S1–S4 for four selected constructs (Figure 7C). For example, the construct attached to the PTC at residue 305 (first cartoon) positions segments S3, S2, and the intervening linker further along the tunnel-translocon complex such that the S2–S3 linker resides in the distal vestibule of the tunnel and compacts. S3 remains extended in the tunnel and S2, completely housed in the translocon, remains compact (likely helical), causing N227 (ΔPTC 79) to be in the translocon and thus unglycosylated. In contrast, the construct attached to the PTC at 325 (third cartoon) positions S2–S4 more distally along the tunnel-translocon pathway. We depict S3, the S2–S3 linker, and S2 as being helical, and S4 as extended near the PTC, thereby locating N227 (ΔPTC 104) at the level of the OST complex. Thus, N227 would be glycosylated similarly to maximal levels achieved for control constructs demonstrated to reach the OST complex[7, 23]. The exact location of each Kv1.3 segment in the tunnel-translocon complex cannot be predicted from the glycosylation assay. However, with the assumption of maintained compaction and the aforementioned caveats, the glycosylation results suggest that native sequences for a variety of transmembrane segments and helical portions of their intervening linkers preferentially acquire secondary structure in the distal vestibule of the ribosomal exit tunnel. Once formed, these structures appear to be retained during their journey through the translocon.

DISCUSSION

Despite recent estimates from structural modeling of the 80 Å anatomical length of the ribosomal tunnel[24], we have evaluated our results throughout this paper in the context of the operational length, ~100 Å, of the tunnel[3, 6]. Accordingly, although there is now ample evidence that compact structures form in the ribosomal exit tunnel near the PTC and the last ~20Å of the tunnel[3–7, 25], much of this evidence derives from a single test sequence inserted into unrelated background sequences. More recently, from a crosslinking study of a transmembrane segment in its native context, it has been suggested that this segment compacts near the PTC and that its secondary structure can influence peptide location in the translocon (Daniel et al, 2008). Do these observations hold for most native helical sequences in their native context? If compaction is modulated by flanking sequences and context, then it is imperative that we investigate native sequences synthesized in the proper sequential order. In this study, we provide further insights into folding of an α-helix inside the tunnel. By systematically lengthening the nascent chain, we now demonstrate that all helical segments in Kv1.3, synthesized in their native order in free ribosomes, compact within the tunnel only in a permissive vestibule near the exit port, and that most compact vectorially from N- to C-terminus as they sequentially enter the distal vestibule.

This conclusion is based on measuring peptide folding in successive locations for identical native chains by moving each transmembrane segment all along the tunnel. Moreover, these experiments probed a variety of strikingly different transmembrane sequences, which allows us to draw general conclusions. For example, S1 is quite hydrophobic vis-à-vis S4 (−12 kcal/mole and −0.2 kcal/mol, respectively, using the Wimley-White hydrophobicity scale). Transmembrane segments S2, S3, and S4 contain charged residues, with S4 having 6 positive charges spaced every third residue apart with intervening neutral, hydrophobic residues. In

addition, these transmembrane segments differ with respect to their translocation/insertion propensities[19]. Isolated S1, S2, and S5 segments individually have strong stop transfer signals and integrate efficiently into the bilayer. In contrast, isolated S3 and S6 segments each behave as secretory proteins, migrating into the ER lumen and do not integrate into the bilayer. The isolated S4 segment is intermediate with an integration efficiency of ~0.5.

While all Kv1.3 transmembrane segments compact in this folding vestibule, they do not do so equivalently. For S1, S3, S4, S5 (this paper), or S6[3], their N-termini compact when they arrive at the distal vestibule while their C-termini, simultaneously located deeper in the tunnel, do not compact until they sequentially enter this vestibule. S2, however, is distinctly different (Figure 3). The N-terminus of S2 never compacts anywhere in the tunnel. Its C-terminus, however, compacts only after the N-terminus has emerged from the tunnel, and all of S2 is compact in the translocon. What accounts for these differences between native transmembrane segments? We speculate that different transmembrane segments of Kv1.3 each have their own unique determinants for helix formation inside the tunnel in the distal vestibule. Some transmembrane segments, e.g. S1, S3, S4, S6, can compact their N-termini without requiring their C-terminus to also be compact. For S2, we speculate that the whole S2 segment behaves as a folding unit. When the N-terminus enters the vestibule, its C-terminus still resides as an extended segment in a non-permissive zone of the tunnel. In this scenario, C-terminal residues do not allow the N-terminus to compact despite its location in the vestibule. When the C-terminus moves to the permissive vestibule, the N- and C-termini each reside in non-restrictive regions and therefore compact. It is possible that the results of Woolhead et al showing that a full-length transmembrane segment (e.g., 24 residues) formed a helix in the tunnel, whereas half of this transmembrane segment (≤ 10 residues) did not[5], are consistent with the existence of a folding unit.

There are two implications for the folding of Kv1.3 transmembrane segments. First, the overall pattern that emerges from the above studies (Figures 2, 4, and Tu et al.6) is that Kv1.3 putative helices only form in the vestibule and do so vectorially from N- to C-terminus as each segment moves sequentially into the vestibule. However, S2 folding may entail a different scenario. Second, transmembrane segments S2, S3, and S4 each compact before completely emerging from the ribosomal exit tunnel. This suggests that although S2–S3–S4 manifests cooperative interactions[6, 19–21, 26], their individual secondary structures are acquired independently. For example, folding of S3 does not require S4 to fold. This suggests that the tertiary folding of the voltage sensor domain occurs via pre-formed secondary structure formation (see below).

Linker Segments

In addition to transmembrane segments, some linker segments of Kv1.3 compact inside the ribosomal tunnel, also in the distal vestibule (see Figure 5). The linking sequences between transmembrane segments have been under-explored and endure a bad track record for structural identification. The reason, of course, is that we tend to think of linkers as flexible disordered regions of polytopic proteins that lack functional roles. However, the crystal structure of a Kv channel chimera[12] indicates short helices in these linker regions. We find that the linkers between S2 and S3 and between S3 and S4 compact and may already contain helices early in their biogenesis, i.e., inside the ribosomal tunnel. In contrast, the atypically long (~39 amino acids) linker between S1 and S2 is extended within the tunnel.

This S1–S2 linker is poorly conserved across Kv channels, which is characteristic of disordered regions. According to the crystal structure of chimera Kv1.2/2.1, the S1–S2 linker has a short helix, which may be a consequence of the channel being a chimera. Tertiary interactions that are normally not present in either Kv1.2 or Kv2.1 may stabilize this short helix. It is possible that tertiary folding/packing drives secondary folding or vice versa. In the S1–S2 linker region, there is only ~20% amino acid identity between Kv1.3 and Kv1.2. Thus, our findings for the

Kv1.3 S1–S2 linker may reflect these non-homologous sequences. Kv2.1, however, does contain a helix in this linker region[16] but has only ~17 amino acids compared to the 39 for Kv1.3 and 37 for Kv1.2. This diversity may underlie idiosyncratic behavior at different stages of assembly and folding. It is also possible that the S1–S2 linker may need to be disordered to promote protein-protein interactions for folding and assembly early in biogenesis, but could form a helix at a later stage for functional purposes (e.g., upon tetramerization or arrival at the plasma membrane). Further experiments are needed to understand the final structure of the S1–S2 linker in Kv1.3.

In addition to structural information regarding the S1–S2 linker, the Kv1.2/2.1 model indicates that a short helix is present in the S2–S3 linker (leading into S3) and the S3–S4 linker (leading into S4)[12]. Our results indicate that these secondary structures may already be manifested early in biogenesis in the distal vestibule of the ribosomal tunnel. If so, then these helices in the S2–S3 linker and in the S3–S4 linker could serve to promote tertiary interactions, which are important during biogenesis. For example, efficient peptide integration into the bilayer may be a function of the stability of the hairpin formed by adjacent transmembrane helices27. This idea is particularly attractive given that S3 and S4 are each weak integrators by themselves19.

We propose that helical linkers present early in biogenesis promote interaction between transmembrane segments S2 and S3 or between S3 and S4 or even between transmembrane segments in the S2–S3–S4 unit as a whole, a putative biogenic intermediate[19–21]. A helix placed at these linker locations serves to shorten the intervening distance between the C-terminus of S2 and the N-terminus of S3 or between the C-terminus of S3 and the N-terminus of S4. Linker helices may stabilize the tertiary structural unit formed by S2–S3–S4. This suggestion is based on observations that linkers serve not only as simple rigid spacers, thereby controlling the distance between domains, but also as a means to prevent unfavorable interdomain interactions[28, 29], and influence the stability, geometry, orientation, and folding rates of helical hairpins[27, 30–34].

Beyond the tunnel

Upon leaving the ribosome, the nascent peptide enters the translocon, and ultimately, for transmembrane segments, the bilayer of the ER. Single transmembrane segments, as well as engineered polyleucines and polyalanines, can compact inside the translocon, as determined by glycosylation assays[7, 23] and FRET measurements[5]. To span the distance from the PTC to the OST complex in the ER lumen requires a chain length of 66–68 residues in an extended conformation[7, 8], equivalent to ~210Å. Based on the results of similar glycosylation assays for Kv1.3 segments in the translocon (Figure 7), we conclude that both transmembrane segments and some linker segments of Kv1.3 not only compact prior to exit of these segments from the ribosomal tunnel, but they also maintain a compact state as they migrate through the translocon.

We cannot, however, completely exclude the possibility that instead of forming α-helices, the region from S2 to S3 may form some random bent structures (hairpin or folded structure) with a similar displacement length along the tunnel-translocon axis during chain elongation. The monotonic pattern of behavior of the chain length-dependent glycosylation (Figure 7) and the agreement of the distance calculations with experimental results, suggest that the most parsimonious explanation is that regions from S2 to S3 remain helical while traversing the tunnel-translocon compartments. These conclusions are consistent with previous studies of a single transmembrane sequence or polyleucine helical sequences[5, 7].

In summary, we conclude native sequences of Kv1.3 that are diversified with all possible natural side-chains (larger, more hydrophobic, or charged) compact only in the last 20Å of the tunnel in free ribosomes. This vestibule is a permissive zone for α-helix formation of Kv1.3

segments. Thus, Kv1.3 helices form sequentially in a vectorial manner (N- to C-terminus) as they enter this zone. Intriguingly, this folding zone has also been shown to accommodate the simplest of tertiary intramolecular interactions in the cytosolic domain of a nascent peptide[35]. To date, we find that sequences that compact near the PTC are also compact in the distal vestibule. However, the corollary is not true. Sequences that compact in the vestibule do not always compact near the PTC.

While we do not know the physicochemical properties of this vestibule that encourage peptide compaction, we may infer that tertiary interactions (with rRNA, riboprotein, or chaperones), electrostatic potential, and decreased water (compared to bulk water), ions, and entropy are contributing, if not dominant, factors[4, 36]. Based on these findings, we speculate that the ribosomal tunnel does not promiscuously permit compaction all along the tunnel for native sequences in a polytopic protein. In addition, the helix formed inside the tunnel remains so while traversing the translocon, which could effectively facilitate subsequent tertiary folding.

Materials and Methods

Constructs and In Vitro Translation

Standard methods of bacterial transformation, plasmid DNA preparation, and restriction enzyme analysis were used. The nucleotide sequences of all mutants were confirmed by automated cycle sequencing performed by the DNA Sequencing Facility at the School of Medicine on an ABI 377 Sequencer using Big dye terminator chemistry (A0BI). pSP/(ΔT1) Kv1.3 was constructed by religation of the *Hind*III/*Nco*I-digested, blunt-ended pSP/Kv1.3/cysteine-free[3]. Engineered cysteines and restriction enzyme sites were introduced into pSP/ΔT1Kv1.3/cysteine-free using QuikChange Site-Directed Mutagenesis Kit. All mutant DNAs were sequenced throughout the entire coding region. Capped cRNA was synthesized in vitro from linearized templates using Sp6 RNA polymerase (Promega, Madison, WI). Linearized templates for Kv1.3 translocation intermediates were generated using several restriction enzymes to produce different length DNA constructs lacking a stop codon (Figure 1B). Proteins were translated in vitro with [^{35}S]Methionine (4 μl/50 μl translation mixture; ~10 μCi/μl Express, Dupont/NEN Research Products, Boston, MA) for 1 hr at 22°C in a rabbit reticulocyte lysate (2 mM final (DTT)) according to the Promega Protocol and Application Guide.

Pegylation Measurements

As described previously[3], translation reaction (40 μl) was added to 500 μl phosphate-buffered saline (PBS, Ca-free, containing 4 mM $MgCl_2$ (pH 7.3)) with 2 mM DTT. The suspension was centrifuged (Beckman Optima TLX Ultracentrifuge, Beckman TLA 100.3 rotor) through a sucrose cushion (100 μl; 0.5 M sucrose, 100 mM KCl, 5 mM $MgCl_2$, 50 mM Hepes, and 1 mM DTT (pH 7.5)) for 20 min at 70,000rpm (~245,000×g) at 4° C to isolate ribosome-bound peptide. The pellet was resuspended on ice in 90 μl of PBS Ca-free buffer containing 4 mM Mg^{2+} and 100 μM DTT (pH 7.3). 10ml buffer containing 10 mM PEG-MAL (5 kDa, Nektar Therapeutics) was added (final PEG-MAL concentration of 1 mM) and incubated at 0°C for two consecutive time points, 3h and 5 h. Reactions were terminated by addition of 100 mM DTT, followed by incubation of the mixture at room temperature for 10–15 min. Samples were collected either by centrifugation at 70,000 rpm at 4° C for 20 min and/or by precipitation with a 90% final volume of cold acid-acetone (900 μl; a stock acid-acetone solution was made by adding 10 μl of HCl to 120 ml acetone). The final sample was mixed with NuPAGE sample buffer and subject to SDS-NuPAGE analysis. The fraction of protein pegylated for each residue was calculated as the ratio of counts per minute in the pegylated band (band 1) to the sum of the counts per minute in the pegylated and unpegylated (band 0) bands. If incompletely translated products were present, then the ratio of the full-length to incompletely translated

products from the control lane (first lane) was used to correct the amount of pegylation of the full-length nascent peptide.

Glycosylation Measurements

Translation reactions (25μl) were performed at 27 °C for ~50 mins in the presence of ~3 μl dog pancreas microsomes (Promega) and then centrifuged through a sucrose cushion at 55,000 rpm for 7 mins at 4°C to isolate membrane-integrated protein in the pellet. The pellet was treated with RNase (2μl of 500 μl/ml stock) before being mixed with loading buffer. For samples treated with dodecylmaloside ($C_{12}M$), the pellet was solubilized with 0.5% $C_{12}M$ on ice for 1~2 hr. Before spinning down the ribosome-attached proteins at 70,000 rpm for 20 mins at 4°C, these samples were pre-centrifuged at 55,000 rpm for 7 mins at 4°C to remove insoluble proteins. The final samples were treated with RNase and mixed with loading buffer before loading on the gel.

Gel Electrophoresis and Fluorography

All final samples were treated with ~2μl of 500 μg/ml RNase for 20 min at room temperature to digest tRNA and remove contaminating peptidyl-tRNA bands. Samples were mixed with NuPAGE sample buffer (1 M glycerol, 0.5 mM EDTA, 73 mM LDS, 141 mM Tris base, and 106 mM Tris-HCl) and heated at 70° C for 10 min before being loaded onto the gel. Electrophoresis was performed using the NuPAGE system and precast Bis-Tris gels and MES (50 mM) or Mops (50 mM) running buffer (50 mM Tris base, 3.5 mM SDS, and 1 mM EDTA). Gels were soaked in Amplify (Amersham Corp., Arlington Heights, IL) to enhance ^{35}S fluorography, dried, and exposed to Kodak X-AR film at −70° C. Typical exposure times were 16–30 h. Quantitation of gels was carried out directly using a Molecular Dynamics (Sunnyvale, CA) PhosphorImager.

Acknowledgments

We thank Dr. Richard Horn, for critical reading of the manuscript.

Supported by National Institutes of Health Grant GM 52302

Abbreviations

PTC	peptidyl transferase center
Kv	voltage-gated K^+
PEG-MAL	polyethylene glycol maleimide

REFERENCES

1. Nissen P, Hansen J, Ban N, Moore PB, Steitz TA. The structural basis of ribosome activity in peptide bond synthesis. Science 2000;289:920–930. [PubMed: 10937990]
2. Kosolapov A, Tu L, Wang J, Deutsch C. Structure Acquisition of the T1 Domain of Kv1.3 During Biogenesis. Neuron 2004;44:295–307. [PubMed: 15473968]
3. Lu J, Deutsch C. Secondary structure formation of a transmembrane segment in Kv channels. Biochemistry 2005;44:8230–8243. [PubMed: 15938612]
4. Lu J, Deutsch C. Folding zones inside the ribosomal exit tunnel. Nat. Struct. Mol. Biol 2005;12:1123–1129. [PubMed: 16299515]
5. Woolhead CA, McCormick PJ, Johnson AE. Nascent membrane and secretory proteins differ in FRET-detected folding far inside the ribosome and in their exposure to ribosomal proteins. Cell 2004;116:725–736. [PubMed: 15006354]

6. Tu L, Wang J, Deutsch C. Biogenesis of the T1-S1 linker of voltage-gated K^+ channels. Biochemistry 2007;46:8075–8084. [PubMed: 17567042]
7. Mingarro I, Nilsson I, Whitley P, von Heijne G. Different conformations of nascent polypeptides during translocation across the ER membrane. BMC Cell Biology 2000;1:3. [PubMed: 11178101]
8. Kowarik M, Kung S, Martoglio B, Helenius A. Protein folding during cotranslational translocation in the endoplasmic reticulum. Molecular Cell 2002;10:769–778. [PubMed: 12419221]
9. Hardesty B, Kramer G. Folding of a nascent peptide on the ribosome. Progress in Nucleic Acid Research & Molecular Biology 2001;66:41–66. [PubMed: 11051761]
10. Daniel CJ, Conti B, Johnson AE, Skach WR. Control of translocation through the Sec61 translocon by nascent polypeptide structure within the ribosome. J. Biol. Chem 2008;283:20864–20873. [PubMed: 18480044]
11. Long SB, Campbell EB, MacKinnon R. Crystal structure of a mammalian voltage-dependent Shaker family K+ channel. Science 2005;309:897–903. [PubMed: 16002581]
12. Long SB, Tao X, Campbell EB, MacKinnon R. Atomic structure of a voltage-dependent K+ channel in a lipid membrane-like environment. Nature 2007;450:376–382. [PubMed: 18004376]
13. Tu L, Santarelli V, Sheng Z-F, Skach W, Pain D, Deutsch C. Voltage-gated K^+ Channels Contain Multiple Intersubunit Association Sites. Journal of Biological Chemistry 1996;271:18904–18911. [PubMed: 8702552]
14. Kobertz WR, Miller C. K^+ channels lacking the `tetramerization' domain: implications for pore structure. Nature Structural Biology 1999;6:1122–1125.
15. Monks SA, Needleman DJ, Miller C. Helical structure and packing orientation of the S2 segment in the Shaker K+ channel. Journal of General Physiology 1999;113:415–423. [PubMed: 10051517]
16. Li-Smerin Y, Hackos DH, Swartz KJ. alpha-helical structural elements within the voltage-sensing domains of a K(+) channel. Journal of General Physiology 2000;115:33–50. [PubMed: 10613917]
17. Aggarwal SK, MacKinnon R. Contribution of the S4 segment to gating charge in the Shaker K+ channel. Neuron 1996;16:1169–1177. [PubMed: 8663993]
18. Seoh, SA.; Sigg, D.; Papazian, DM.; Bezanilla, F. Voltage-sensing residues in the S2 and S4 segments of the *Shaker* K^+ channel. 1996. p. 1159-1167.
19. Tu L, Wang J, Helm A, Skach WR, Deutsch C. Transmembrane biogenesis of Kv1.3. Biochemistry 2000;39:824–836. [PubMed: 10651649]
20. Sato Y, Sakaguchi M, Goshima S, Nakamura T, Uozumi N. Molecular dissection of the contribution of negatively and positively charged residues in S2, S3, and S4 to the final membrane topology of the voltage sensor in the K+ channel, KAT1. J. Biol. Chem 2003;278:13227–13234. [PubMed: 12556517]
21. Zhang L, Sato Y, Hessa T, von HG, Lee JK, Kodama I, Sakaguchi M, Uozumi N. Contribution of hydrophobic and electrostatic interactions to the membrane integration of the Shaker K+ channel voltage sensor domain. Proc. Natl. Acad. Sci. U. S. A 2007;104:8263–8268. [PubMed: 17488813]
22. Zhu J, Watanabe I, Poholek A, Koss M, Gomez B, Yan C, Recio-Pinto E, Thornhill WB. Allowed N-glycosylation sites on the Kv1.2 potassium channel S1–S2 linker: implications for linker secondary structure and the glycosylation effect on channel function. Biochem. J 2003;375:769–775. [PubMed: 12911333]
23. Whitley P, Nilsson IM, von Heijne G. A nascent secretory protein may traverse the ribosome/endoplasmic reticulum translocase complex as an extended chain. J. Biol. Chem 1996;271:6241–6244. [PubMed: 8626416]
24. Voss NR, Gerstein M, Steitz TA, Moore PB. The geometry of the ribosomal polypeptide exit tunnel. J. Mol. Biol 2006;360:893–906. [PubMed: 16784753]
25. Woolhead CA, Johnson AE, Bernstein HD. Translation arrest requires two-way communication between a nascent polypeptide and the ribosome. Mol. Cell 2006;22:587–598. [PubMed: 16762832]
26. Papazian DM, Shao XM, Seoh SA, Mock AF, Huang Y, Wainstock DH. Electrostatic interactions of S4 voltage sensor in Shaker K+ channel. Neuron 1995;14:1293–1301. [PubMed: 7605638]
27. Wehbi H, Rath A, Glibowicka M, Deber CM. Role of the extracellular loop in the folding of a CFTR transmembrane helical hairpin. Biochemistry 2007;46:7099–7106. [PubMed: 17516627]

28. Arai R, Ueda H, Kitayama A, Kamiya N, Nagamune T. Design of the linkers which effectively separate domains of a bifunctional fusion protein. Protein Eng 2001;14:529–532. [PubMed: 11579220]

29. George RA, Heringa J. An analysis of protein domain linkers: their classification and role in protein folding. Protein Eng 2002;15:871–879. [PubMed: 12538906]

30. Engel DE, DeGrado WF. Alpha-alpha linking motifs and interhelical orientations. Proteins 2005;61:325–337. [PubMed: 16104016]

31. van Leeuwen HC, Strating MJ, Rensen M, de LW, van der Vliet PC. Linker length and composition influence the flexibility of Oct-1 DNA binding. EMBO J 1997;16:2043–2053. [PubMed: 9155030]

32. Robinson CR, Sauer RT. Optimizing the stability of single-chain proteins by linker length and composition mutagenesis. Proc. Natl. Acad. Sci. U. S. A 1998;95:5929–5934. [PubMed: 9600894]

33. Kostakioti M, Stathopoulos C. Role of the alpha-helical linker of the C-terminal translocator in the biogenesis of the serine protease subfamily of autotransporters. Infect. Immun 2006;74:4961–4969. [PubMed: 16926387]

34. Johnson CP, Gaetani M, Ortiz V, Bhasin N, Harper S, Gallagher PG, Speicher DW, Discher DE. Pathogenic proline mutation in the linker between spectrin repeat: disease caused by spectrin unfolding. Blood 2007;109:3538–3543. [PubMed: 17192394]

35. Kosolapov A, Deutsch C. Tertiary interactions within the ribosomal exit tunnel. Nat. Struct. Mol. Biol 2009;16:405–411. [PubMed: 19270700]

36. Lu J, Kobertz WR, Deutsch C. Mapping the electrostatic potential within the ribosomal exit tunnel. J. Mol. Biol 2007;371:1378–1391. [PubMed: 17631312]

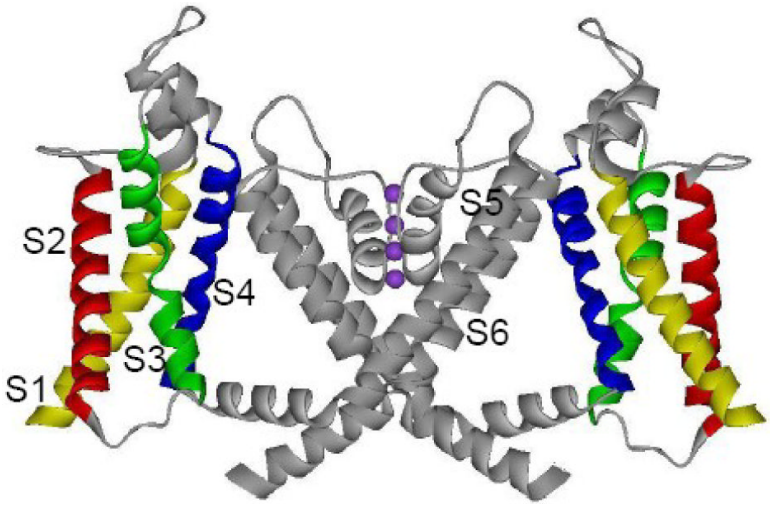

Figure 1. Structure of Kv1.2/Kv2.1 chimera

A ribbon representation of two opposing subunits of Kv1.2/Kv2.1 was made in DS ViewerPro (www.accelrys.com) from Long et al.[12]. Four K^+ ions in the selectivity filter are shown as purple spheres. The transmembrane segments, S1, S2, S3, S4 are shown as yellow, red, green, and blue ribbons, respectively, and S5, S6 and the pore helix are depicted as gray ribbons.

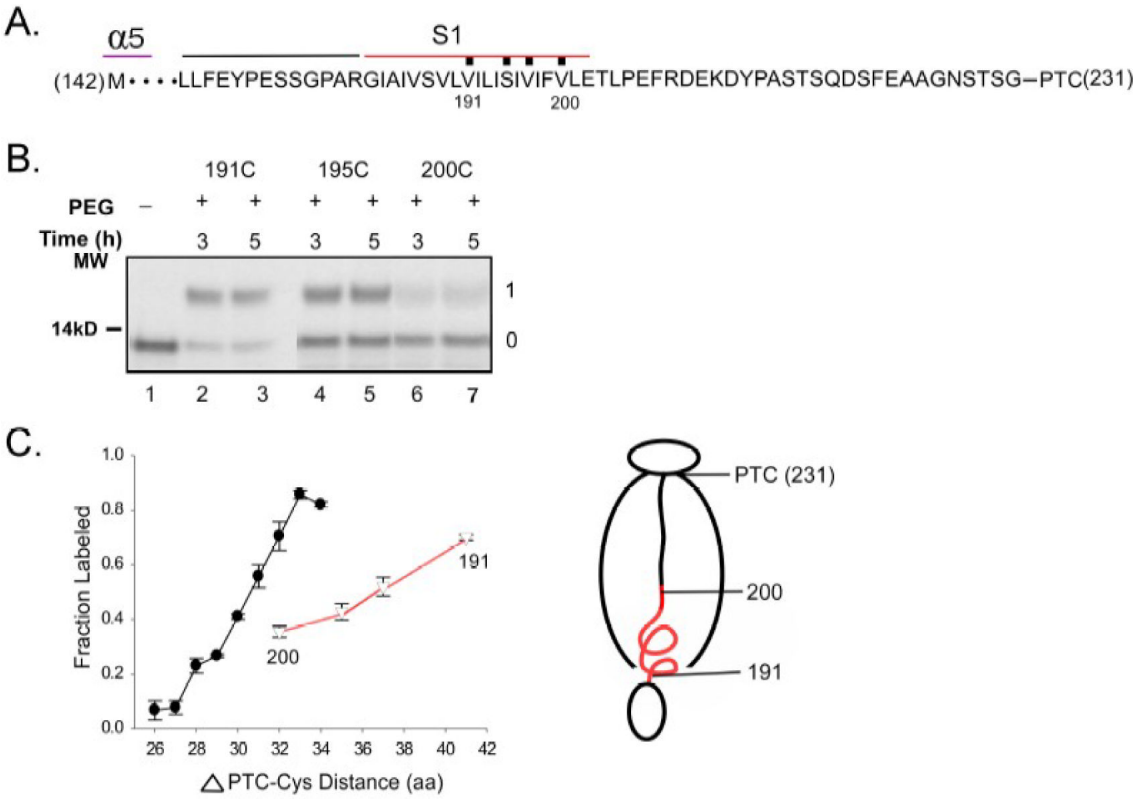

Figure 2. C-terminal segment of S1 in the tunnel

(A) The primary sequence of S1 and flanking sequences. The amino acid sequence is indicated by a single-letter code. Long stretches of amino acids present in the construct but omitted from the diagrammed sequence are indicated by ellipses (….). The filled squares above selected amino acids represent residues mutated, one at a time, to cysteine. A restriction enzyme was used to truncate the peptide at residue 231, which remains attached to tRNA at the PTC. The start site of all T1-deleted Kv1.3 constructs is 142. The number under the letter code corresponds to the amino acid in the native full-length sequence in Kv1.3 used to generate the indicated ΔPTC values. Different segments of Kv1.3 are labeled above the corresponding sequence. **(B)** Pegylation of S1 C-terminal region. Nascent peptides were pegylated and fractionated on polyacrylamide gels as described in the Methods. The first lane, derived from a sample not treated with PEG-MAL, was used as the zero time point. Lanes 2–7 for each indicated cysteine residue show samples incubated with 1mM PEG-MAL for 3 and 5h. Gels were 12% NuPAGE Bis-Tris gels with MES running buffer. The number to the left of the gel is a molecular weight standard; numbers to the right of the gel indicate unpegylated (0) and singly pegylated (1) protein. **(C)** Fraction of nascent peptide labeled. The x-axis is the number of amino acids from the PTC site to (and including) the labeled cysteine. Pegylation of a known extended peptide, the tape measure is shown by the filled circles and represents data taken from Lu and Deutsch[3]. The final extent of pegylation of individual residues in the C-terminus of S1 is represented by the open triangles. Data are means ± SEM ($n \geq 3$). The cartoon next to the plot depicts the ribosome with the nascent peptide, indicating the PTC, and, in red, the segment scanned and pegylated. Secondary structure is indicated by the helical drawing of the red line. The N-terminal portion of the nascent peptide that resides outside of the tunnel is represented as a circle below the ribosome because its structure outside the tunnel is unknown.

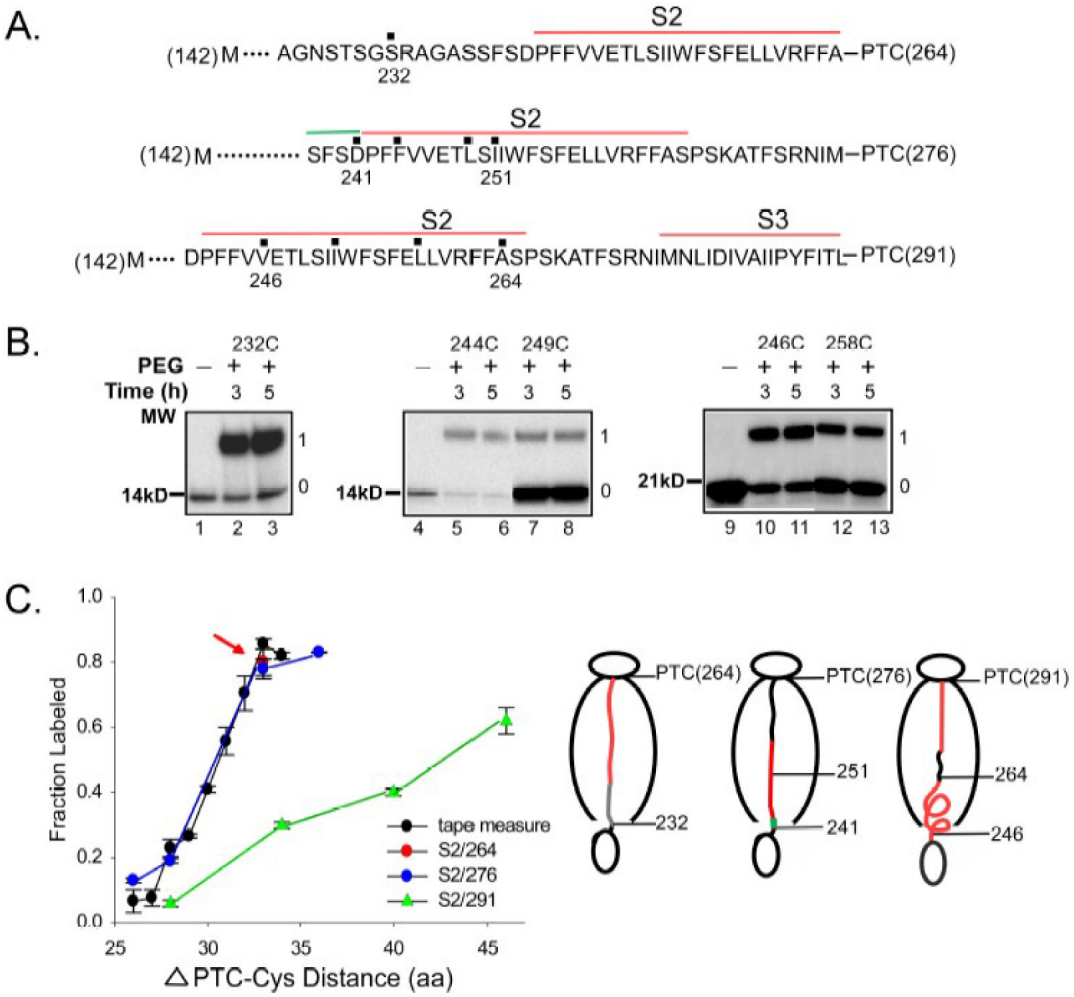

Figure 3. The S2 transmembrane segment in the tunnel

(A) The primary sequences, as described for Figure 2A, are shown for the *Nhe*I (264)-cut construct, the *BspH*I (276)-cut construct, and the *Kpn*I (291)-cut construct. **(B)** Pegylation of S2 residues. The gels are as described in Figure 2C. **(C)** Fraction of nascent peptide labeled. The final extent of pegylation of S2 residues in the (264)-cut construct is shown as the red circle (highlighted by arrow), the (276)-cut construct, as blue circles, and the (291)-cut construct, as green triangles. Data are means ± SEM for triplicate samples. Each cartoon, as described in figure legend 2C, depicts the cut-site at the PTC, the region scanned, and an interpretation of the data: the peptide region scanned is extended for the constructs cut at 264 and 276, but compact for the construct cut at residue 291.

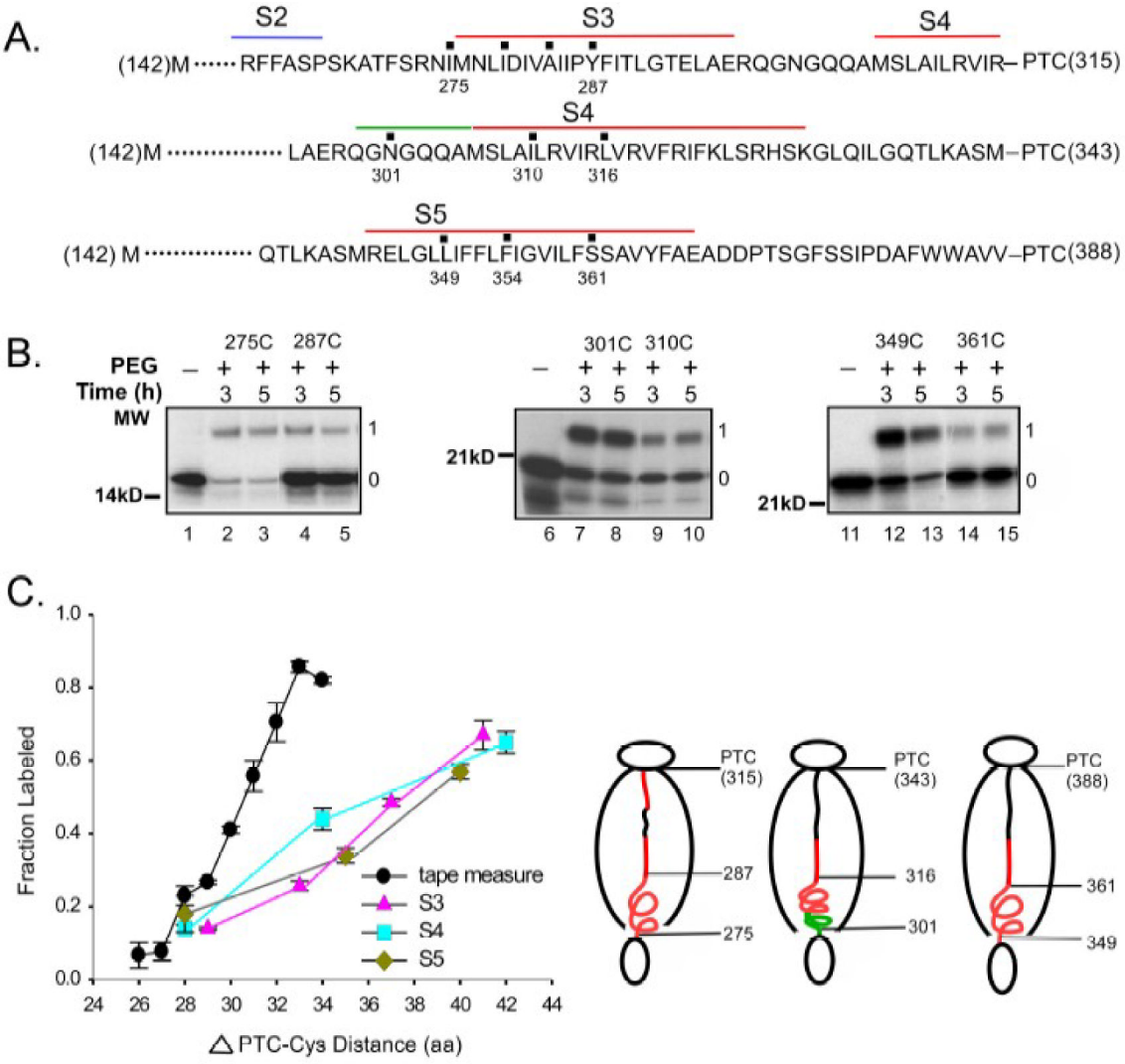

Figure 4. Transmembrane segments S3, S4, and S5 in the tunnel

(A) The primary sequences of constructs for probing the secondary structure of S3 (*Nsi*I (315)-cut construct), S4 (*Xcm*I (343)-cut construct), and S5 (*BstE*II (388)-cut construct). **(B).** Fraction of peptide labeled. For each transmembrane segment, S3–S5, the tested cysteines are indicated by red, green, and tan symbols, respectively, and plotted along with the length-dependent pegylation for the tape measure (solid black circles). Data are means ± SEM for triplicate samples. The cartoon, as described in figure legend 2C, depicts the cut-site at the PTC, the region scanned, and an interpretation of the data: In each case, the peptide region scanned is compact (likely α-helical).

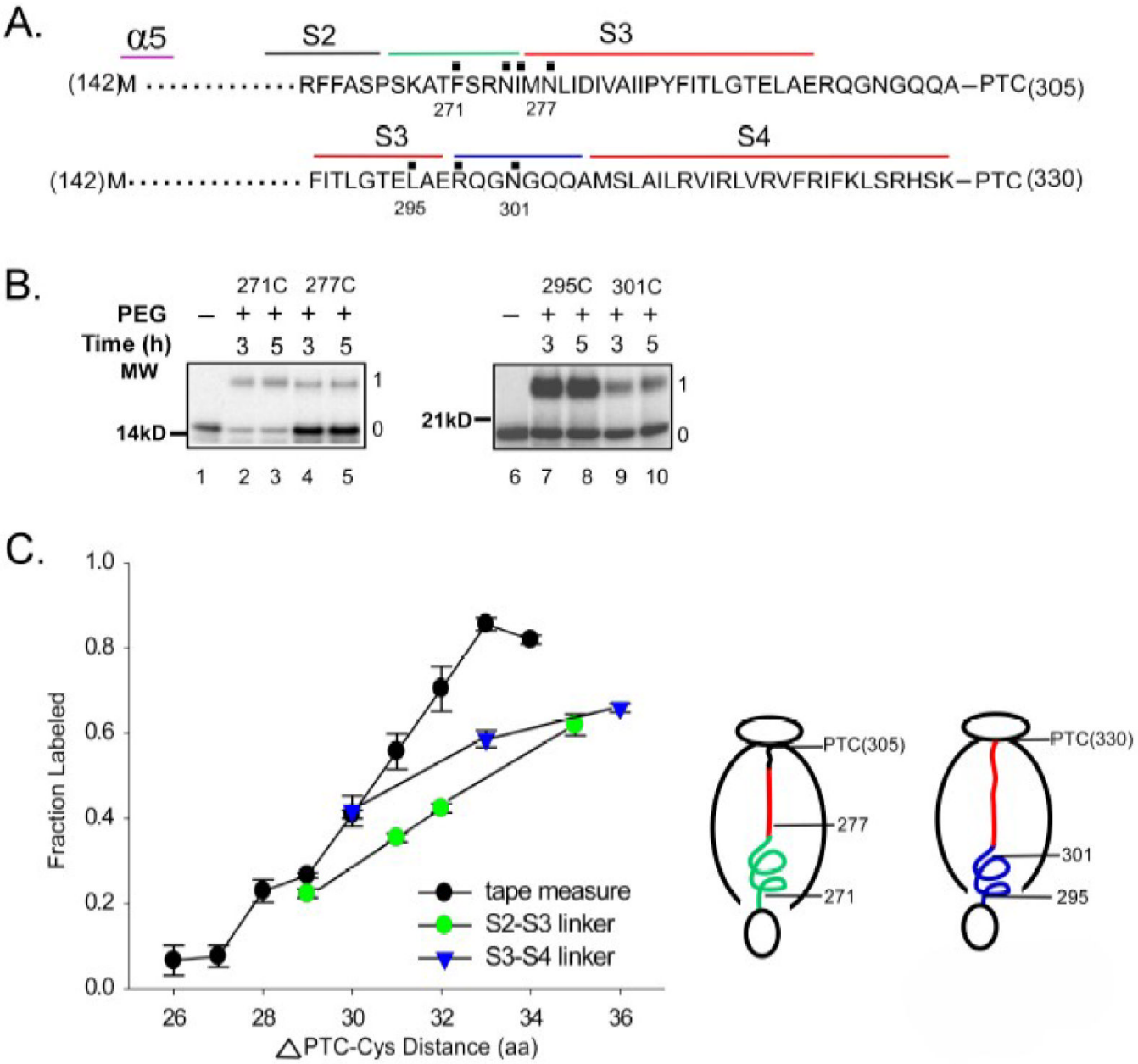

Figure 5. The S2–S3 and S3–S4 linkers in the tunnel

(A) The primary sequences are shown for the *Bst*XI (305)-cut construct and the *Sty*I (330)-cut construct. **(B).** Fraction of peptide labeled for the S2–S3 (green circles) and S3–S4 (blue triangles) linkers. The length-dependent pegylation for the tape measure is shown as filled black circles. Data are means ± SEM for triplicate samples. In some cases, the SEM values are smaller than the symbol. The cartoons, as described in figure legend 2C, depict the cut-sites at the PTC (305 and 330, respectively), the region scanned (271–277 and 295–310, respectively), and interpretations of the data: The S2–S3 linker scanned is compact (likely α-helical), as is the S3–S4 linker region scanned

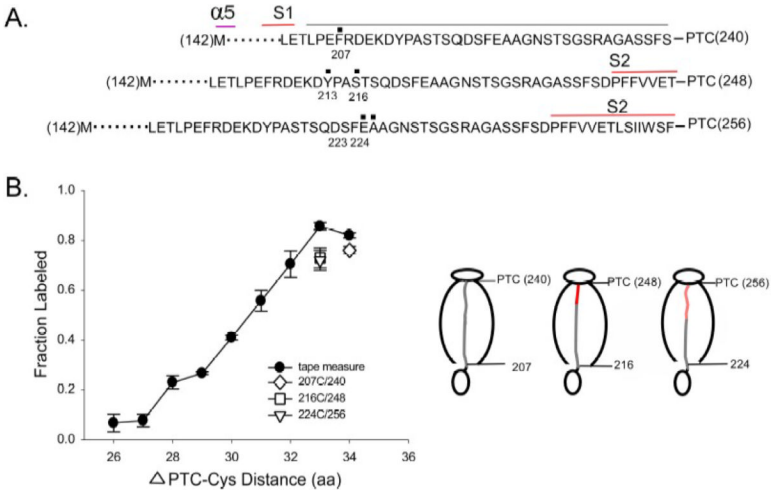

Figure 6. The S1–S2 linker in the tunnel

(A). The primary sequences of the S1–S2 linker located in three different tunnel locations. **(B).** Fraction of nascent peptide labeled. The final extent of pegylation of individual S1–S2 linker residues is represented by the open diamond (207C), square (216C), and inverted triangle (224C) in constructs with residues 240, 248, and 256, respectively, at the PTC. The all-extended tape measure is shown as black circles. Data are means ± SEM for triplicate samples. The cartoons, as described in figure legend 2C, depict peptides generated by different cut-sites at the PTC, the respective cysteines tested (range of ΔPTC is 33–34), and an interpretation of the data: The S1–S2 loop is extended in every location in the tunnel.

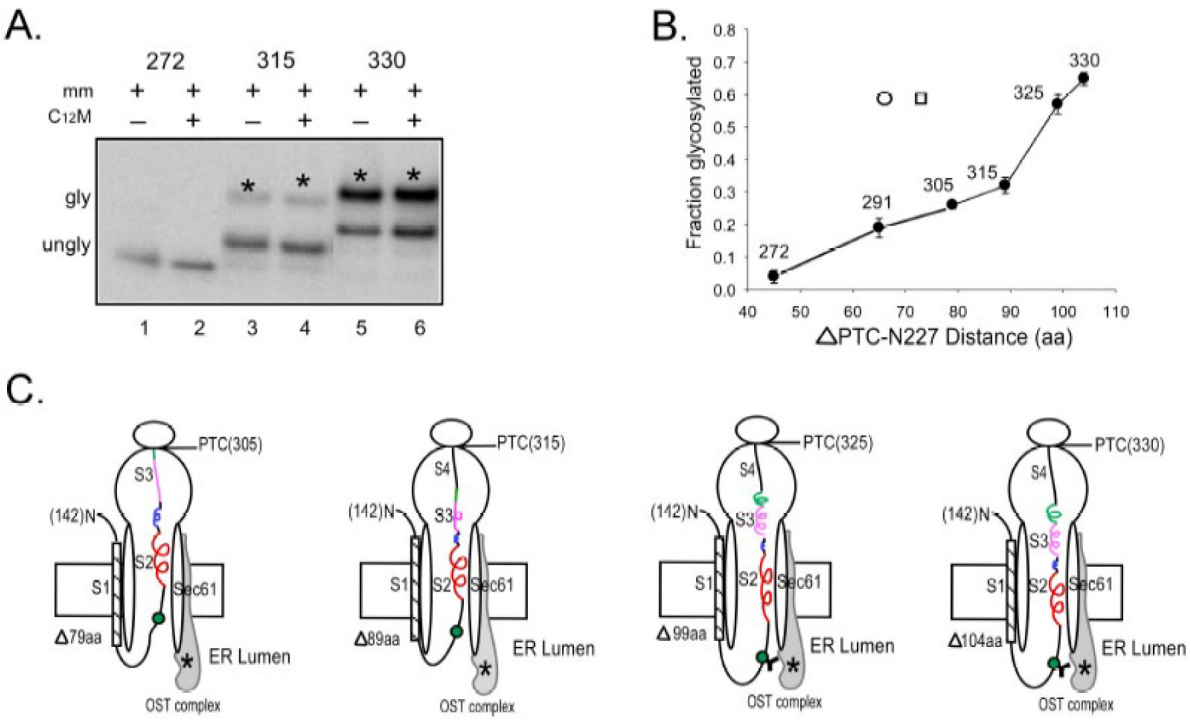

Figure 7. Helices inside the translocon

(A). Glycosylation of nascent peptide. Constructs of various lengths (ΔPTC-N227) were translated as described previously but in the presence of microsomal membranes (mm) and glycosylation of the nascent peptide asparagine residue, N227, was evaluated by gel fractionation using a 4–12% NuPAGE Bis-Tris gel for the constructs indicated. The numbers 272, 315, and 330 represent the residue that remains attached to the tRNA at the PTC. The lower band in each lane indicates unglycosylated peptide. The upper band (marked by an asterisk) in each lane indicates peptide glycosylated by the oligosaccharyltransferase complex in the ER lumen. **(B).** Extent of glycosylation. The fraction glycosylated was calculated from the $C_{12}M$-treated samples (lanes 2, 4, 6) as the cpm in the upper band divided by the sum of cpm in the upper and lower bands, and plotted as a function of distance in amino acids from the PTC, ΔPTC-N227. According to von Heijne and co-workers[7], a peptide that is all extended in the ribosome-translocon complex achieves maximal glycosylation at a chain length of ~66 from the PTC to the asparagine (open circle), whereas a compact peptide control containing 17 leucines is maximally glycosylated at a chain length of ~74 from the PTC to the asparagine (open square). Data are means ± SEM for triplicate measurements. **(C).** Cartoon representations of the ribosome-translocon complex with different length peptides based on results from Figures 2–5 and 7B. Segments depicted are S2 (red line), S2–S3 linker (blue line), S3 (pink line), S3–S4 linker (green line) and S4 (black line). A helical versus extended conformation is suggested by the line shape. The green circle represents N227, which is glycosylated (Y-shaped black symbol) in the third and fourth cartoons (PTC 325 and 330). The OST complex (gray) includes the oligosaccharyltransferase enzyme that resides in the ER lumen and the asterisk indicates the active site of the enzyme. The translocon (elongated white ovals) is labeled as Sec61. Each different restriction site (305, 315, 325, 330) produces a different ΔPTC-N227 (labeled as Δ79, Δ89, Δ99, Δ104, respectively) and relocates S2, S3, and S4 in the ribosome-translocon complex as indicated, according to the assumptions/caveats stated in the text. The relative lengths of transmembrane and linker segments are not to scale.